EUROPEAN ORGANIZATION FOR NUCLEAR RESEARCH

HIE-ISOLDE-PROJECT-Note-0005

Second-order Transit Time Factors for a Two Gap Resonator

M.A. Fraser

Abstract

The HIE-ISOLDE linac at CERN will operate independently phased quarter-wave resonators (QWRs) in order to accelerate radioactive ion beams (RIBs), with mass to charge states in the range $2.5 < A/q < 4.5$, from 1.2 MeV/u up to an energy of at least 10 MeV/u. The low-β version of the QWR will also be used to decelerate beams below 1.2 MeV/u. The combination of low velocity and high gradient results in a significant change of the ion velocity and a breakdown of the first-order approximation commonly used to calculate the energy gain in accelerating cavities. The first-order transit-time factor for two gaps is briefly reviewed before higher-order transit-time factors are derived and the energy gain expressed, taking into account the variation in velocity, to second-order. The formalism of J.R. Delayen, introduced in [1], is used throughout.

HIE-ISOLDE-PROJECT-Note-0005
31 Oct 2009

Geneva, Switzerland

October 2009

Contents

1 Introduction

In the baseline design for the HIE-ISOLDE linac the velocity of the beam can change by up to 10 % in each quarter-wave resonator (QWR) immediately after injection, see [2]. Although the energy gain integrated along the whole linac in the baseline case varies by just a few percent with respect to the first-order approximation, the phasing of the QWRs cannot not be calculated accurately without taking into account the effect of the velocity change, especially if the cavities are used to decelerate the beam significantly below the geometric velocity. Accurately tuning the phases of the QWRs in the realistic field simulations is critical in order to correctly model the transverse defocusing force acting on the beam; using numerical methods to tune the linac is computer intensive and time consuming. The second-order approximation of the energy gain presented here allows for a fast and accurate method of tuning. It is also an extremely powerful tool for calculating the energy gain and understanding the stability of the beam at velocities below the geometric velocity of the QWR. It is foreseen to fully exploit the flexibility of the independently phased linac and to decelerate RIBs to below 1.2 MeV/u, offering an even wider range of beam energies at ISOLDE. In this scenario, the second-order approximation will be useful in understanding the beam dynamics at low velocities and tuning the voltages and phases of the QWRs. The formalism used to derive the second-order transit-time factors is that of J.R. Delayen, which is explained in [1]. Most of what follows is consistent with the referenced notation, however, it should be noted that the expression for the first-order transit-time factor $\hat{T}(\beta)$ used in this report includes both the reduction in energy gain from the sinusoidal time dependence of the accelerating field and from the difference of the ion velocity from the optimum velocity. Therefore, $\hat{T}$ is related to the normalised transit-time factor $T(\beta)$ as,

$$\hat{T}(\beta) = \Theta T(\beta),$$

where,

$$\Theta = \frac{\mathrm{Max} \int_{-\infty}^{+\infty} E(z) \sin\left(\frac{2\pi z}{\beta\lambda}\right) \mathrm{d}z}{\Delta V_0},$$

and the equivalent voltage of the resonator in the electrostatic case is,

$$\Delta V_0 = \int_{-\infty}^{+\infty} |E(z)| \, \mathrm{d}z.$$

2 Energy Gain Calculated Numerically

The energy gain ΔW of an ion with charge q and reduced velocity β interacting with an rf electric field E can be calculated by the line integral,

$$\Delta W = q \int_{-\infty}^{+\infty} E(z) \sin\left(\psi(z) + \phi\right) \mathrm{d}z, \tag{1}$$

where the harmonically varying accelerating field is in the z direction and ϕ is the phase when the particle would cross the origin ($z = 0$) in the absence of acceleration. The phase of the field seen by the particle can be written in terms of its position along the z-axis using the following relationship,

$$\psi(z) = \frac{2\pi}{\lambda} \int_{z_i}^{z} \frac{\mathrm{d}z}{\beta(z)} + \psi(z_i), \tag{2}$$

where the integral starts at an initial position z_i outside of the influence of the electric field of the cavity, i.e.,

$$\psi(z_i) = \frac{2\pi z_i}{\beta(z_i)\lambda}. \tag{3}$$

λ is the wavelength of the rf oscillations of the electric field and ϕ is often referred to as the synchronous phase if the coordinate origin is positioned at the symmetry point in the centre of the accelerating gap or cavity.

The calculation should be done numerically and the change in the velocity followed at every step of the integration. The numerical method can be used to calculate the energy gain with the realistic electromagnetic fields of the resonator, themselves calculated using specialised electromagnetic field solvers. The integration must be repeated every time any of the parameters in the equation are varied, e.g. A, q, ΔV_0 or β.

3 Energy Gain at First-order

The energy gain at first-order is calculated by assuming that the ion velocity is constant in the resonator, allowing the variables of phase and velocity to be separated as shown,

$$\Delta W = q\Delta V_0 \hat{T}(\beta)\cos\phi.$$

The energy gain will be derived for an ideal two gap resonator in which the accelerating field is constant within the gaps, i.e. in the 'hard-edge' or 'square-wave' approximation, as shown in Figure 1.

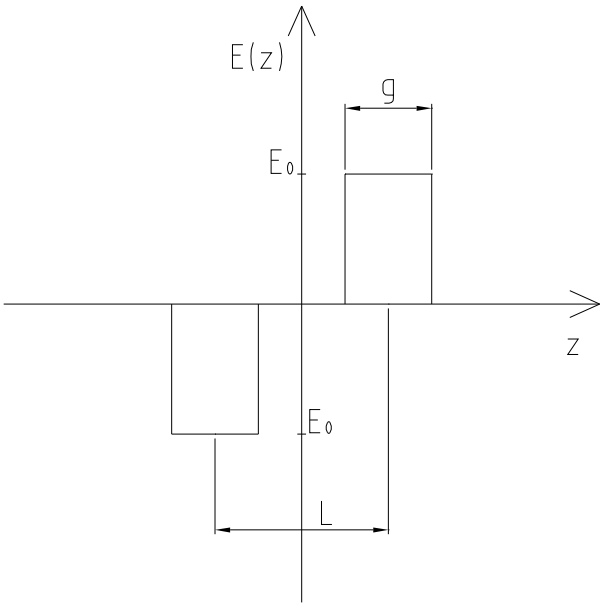

Figure 1: The accelerating electric field configuration used to calculate the energy gain in the first-order approximation.

In this case, the transit-time factor can be expressed as,

$$\hat{T}_{2\,gap}(\beta) = \frac{\beta\lambda}{\pi g}\sin\frac{\pi g}{\beta\lambda}\sin\frac{\pi\beta_g}{2\beta}, \tag{4}$$

where,

$$L = \frac{\beta_g\lambda}{2}.$$

In the thin gap limit, i.e. $g \ll \beta_g\lambda/2$, the transit-time factor is maximised at the geometric velocity of the cavity, i.e. $\hat{T}_{2\,gap}|_{max} = \hat{T}_{2\,gap}(\beta_g)$. This is not the case in a real resonator where the maximum velocity of the transit-time factor, commonly known as the optimum velocity β_0 must be determined numerically from,

$$\frac{\mathrm{d}}{\mathrm{d}\beta}\hat{T}_{2\,gap}\bigg|_{\beta=\beta_0} = 0.$$

One can introduce a scaling factor ξ which is dependent on the gap size, such that β_0 can be represented in the transit-time factor, as shown,

$$\hat{T}_{2\,gap}(\beta) = \frac{\beta\lambda}{\pi g}\sin\frac{\pi g}{\beta\lambda}\sin\frac{\pi\beta_0}{2\xi\beta}, \tag{5}$$

where,

$$\beta_0 = \xi\beta_g.$$

The details of such a formalism and the behaviour of ξ as a function of g is detailed in [1].

3.1 Example: the HIE-ISOLDE high-β QWR

In a real resonator the accelerating field has a more complicated spatial structure, owing to the resonator's geometry and the presence of beam ports. Therefore, in order to apply this formalism to a realistic field, the transit-time factor is calculated numerically and the parameters representing the effective gap length and geometric velocity are attained by fitting the analytic first-order expression in Equation 4 to the numerical data. The transit-time factor is an intrinsic property of a resonator and although this procedure is numerical it only needs carrying out once. An example of such a fit is shown in Figure 2 for the HIE-ISOLDE high-β QWR. The effective parameters calculated from the fit are compared to the mechanical parameters of the QWR in Table 1. For the high-β QWR $\xi = 1.09$ and hence $\beta_0 = 11.3$ %.

Table 1: The fitted parameters for the first-order transit-time factor with the realistic accelerating field of the HIE-ISOLDE high-β QWR.

Parameter	**Mechanical (geometric) Value**	**Fitted (effective) Value**
g (cm)	7.0	7.9
L (cm)	16.0	15. 3
β_g (%)	10.8	10.4

The hard-edge approximation fits the numerical data well, however, below a velocity of about 4 % the approximation poorly predicts the first-order transit-time factor of the realistic field in the HIE-ISOLDE high-β QWR.

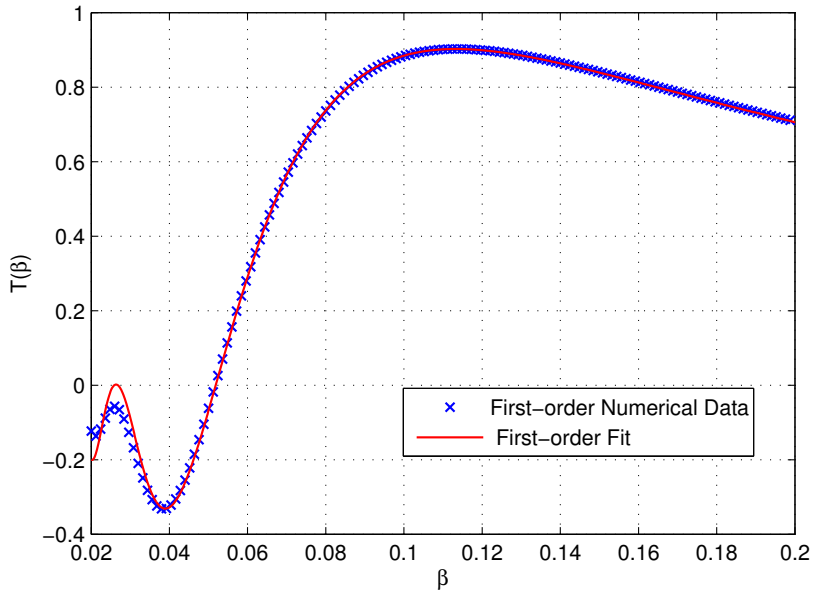

Figure 2: The first-order transit-time factor $\hat{T}_{2\,gap}(\beta)$ calculated numerically and fitted with the analytic approximation. The fitted parameters can be found in Table 1.

4 Energy Gain at Second-order

When a small change of velocity is considered in the cavity, the energy gain can be expressed to second-order as,

$$\Delta W = q\Delta V_0 \hat{T}(\beta)\cos\phi + \frac{(q\Delta V_0)^2}{W}(\hat{T}^{(2)}(\beta) + \hat{T}_s^{(2)}(\beta)\sin 2\phi), \tag{6}$$

where W is the kinetic energy and two second-order transit-time functions, $\hat{T}^{(2)}(\beta)$ and $\hat{T}_s^{(2)}(\beta)$, are introduced in order to separate the coupled phase and velocity dependence. The second-order transit-time factors are also intrinsic to the resonator and are related to the first-order transit-time factor as shown,

$$\hat{T}^{(2)}(x) = -\frac{x}{4}\hat{T}(x)\hat{T}'(x), \tag{7}$$

$$\hat{T}_s^{(2)}(x) = -\frac{x}{8\pi}\int_{-\infty}^{+\infty} \frac{\hat{T}'(x+x')\hat{T}(x-x') - \hat{T}(x+x')\hat{T}'(x-x')}{x'}\,\mathrm{d}x', \tag{8}$$

where,

$$\hat{T}'(x) = \frac{\mathrm{d}}{\mathrm{d}x}\hat{T}(x).$$

Equations 6, 7 and 8 are derived in [1]. Using these expressions the corresponding analytic second-order transit-time factors for a two gap resonator in the 'square-wave' approximation were derived:

$$\hat{T}_{2\,gap}^{(2)}(\beta) = -\frac{\hat{T}_{2\,gap}(\beta)}{4}\left[\cos\frac{\pi g}{\beta\lambda}\sin\frac{\pi\beta_g}{2\beta} + \frac{\beta_g\lambda}{2g}\sin\frac{\pi g}{\beta\lambda}\cos\frac{\pi\beta_g}{2\beta} - \hat{T}_{2\,gap}(\beta)\right],$$

$$\hat{T}^{(2)}_{s,2\,gap}(\beta) = \frac{\pi\beta_g}{16\beta}\hat{T}^2_{1\,gap}(\beta) + \frac{\beta\lambda}{16\pi g}\cos\frac{\pi\beta_g}{\beta}\left[\hat{T}_{1\,gap}\left(\frac{\beta}{2}\right) - 1\right],$$

where,

$$\hat{T}_{1\,gap}(\beta) = \frac{\beta\lambda}{\pi g}\sin\frac{\pi g}{\beta\lambda}.$$

The complete derivations of $\hat{T}^{(2)}_{2\,gap}(\beta)$ and $\hat{T}^{(2)}_{s,2\,gap}(\beta)$ are shown in Appendices A and B, and the relevant standard integrals are collected in Appendix D.

4.1 Example: the HIE-ISOLDE low-β QWR

The transit-time factor for the HIE-ISOLDE low-β cavity is shown in Figure 3 using the realistic field and using the analytic square-wave approximation.

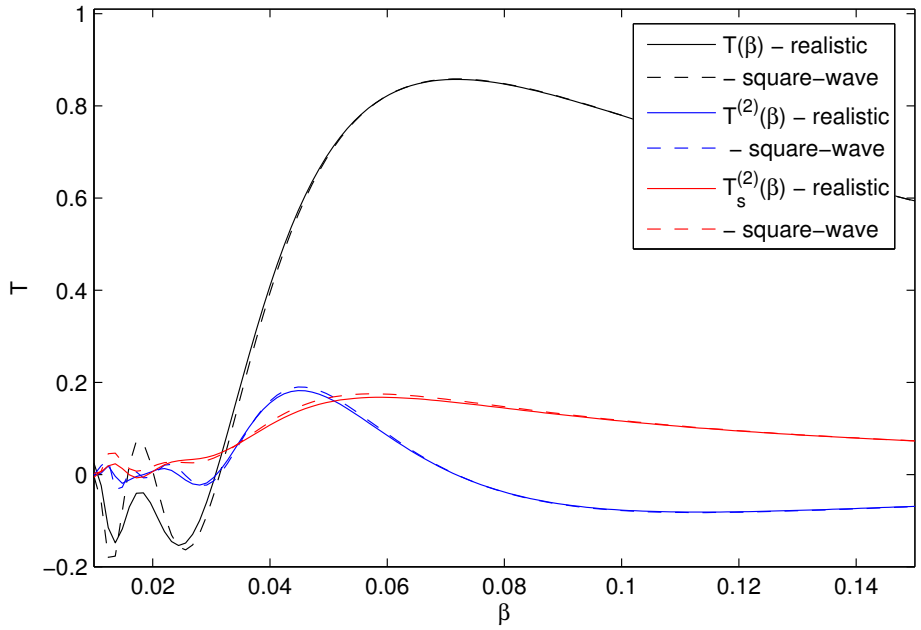

Figure 3: The first and second-order transit-time factors for the HIE-ISOLDE low-β QWR.

The validity of the analytic approximation was investigated at low velocity. The differences between the transit-time factors of the low-β cavity produced using the realistic field profile and those produced with the analytic square-wave field are compared in Figure 4.

For $\beta \gg \beta_g$ the square-wave field approximates very well the realistic field and the difference is negligible. The second-order transit-time factors are well described by the analytic expressions derived using the square-wave approximation and it is the first-order transit-time factor that is most sensitive to the shape of the field at low velocity. Therefore, it is the first-order transit-time factor that limits the use of the square-wave analytic approximation for accurate calculations of the energy change in the low-β cavity below its geometric velocity.

The second-order approximation can be effectively applied if the realistic field profile is used to generate the transit-time factors and is accurate to a few percent down to $\beta_g/3$, below which higher-order approximations are required. All transit-time factors used in the following calculations were derived numerically with the realistic field profile, using the equations described in the Appendix of [1].

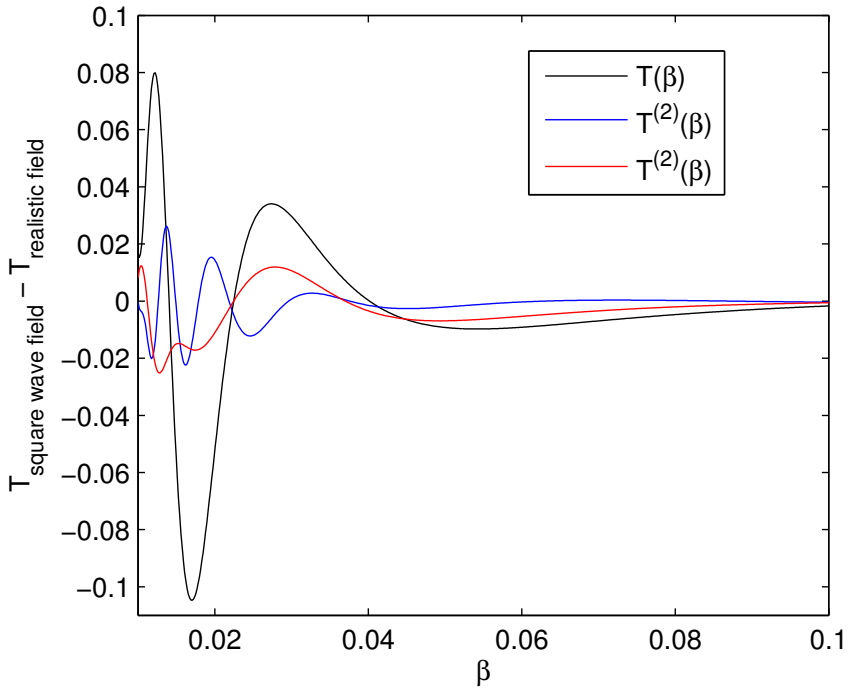

Figure 4: Difference between transit-time factors of the low-β cavity calculated using the realistic field profile and the square-wave approximation.

5 Characteristics of Deceleration Below β_g

From the second-order analytic expression for the energy change in an accelerating cavity given in Equation 6, one can discern a few characteristics of the longitudinal beam dynamics when decelerating in a linac composed of short and independently phased resonators:

- All three transit-time factors $\hat{T}$, $\hat{T}^{(2)}$ and $\hat{T}_s^{(2)}$ are positive in the velocity range $\beta_g/2 < \beta < \beta_g$.
- In this velocity range the rate of deceleration and the effective potential available for deceleration is reduced with respect to the first-order expression in the phase-stable region of $-\pi < \phi < -\pi/2$.
- It is possible to decelerate through the zero of $\hat{T}$.
- The phase dependence of the energy gain is not sinusoidal at low velocity and the extrema of ΔW versus ϕ vary significantly from first-order estimates.

5.1 Phasing the QWR

Phase-stable deceleration through the zero of the first-order transit-time factor is possible by smoothly varying the synchronous phase from the within the range $-\pi < \phi < -\pi/2$ to the range $-5\pi/4 < \phi <$

$-\pi$ as the $\sin 2\phi$ term dominates close to $\beta_g/2$, requiring a phase shift of $\pi/2$. The phase must then be switched rapidly by π into the range $-\pi/2 < \phi < 0$ and eventually into the range $0 < \phi < \pi/2$ as the sign of the first-order transit-time factor switches and starts to dominate again below $\beta_g/2$. The above listed regions of phase stability that are compatible with deceleration are shown in bold in the schematic of Figure 5(a) and the shifting phase of the minimum of the energy gain shown in Figure 5(b). The shift in phase required to maintain the longitudinal phase stability of the beam can be described analytically by calculating the extrema of the second-order approximation for the energy gain. From setting the derivative with respect to ϕ to zero,

$$\left.\frac{\partial W}{\partial \phi}\right|_{\phi=\phi_{\Delta W_{\min}}} = -q\Delta V_0 T(\beta)\sin\phi_{\Delta W_{\min}} + \frac{2(q\Delta V_0)^2}{W} T_s^{(2)}(\beta)\cos 2\phi_{\Delta W_{\min}} = 0, \tag{9}$$

one can write the phase at which the energy gain is minimised as,

$$\phi_{\Delta W_{\min}}(\beta) = \arcsin\left(\frac{\pm\sqrt{1+32\left(\frac{q\Delta V_0}{W}\right)^2\left(\frac{T_s^{(2)}(\beta)}{T(\beta)}\right)^2}-1}{8\left(\frac{q\Delta V_0}{W}\right)\frac{T_s^{(2)}(\beta)}{T(\beta)}}\right), \tag{10}$$

where the root should be chosen depending on the velocity of the particle. The phase of the minimum in the second-order approximation is compared to numerical calculations in Figure 5(b), alongside the schematic illustrating the phase shifts. The phase independent term of the second-order approximation

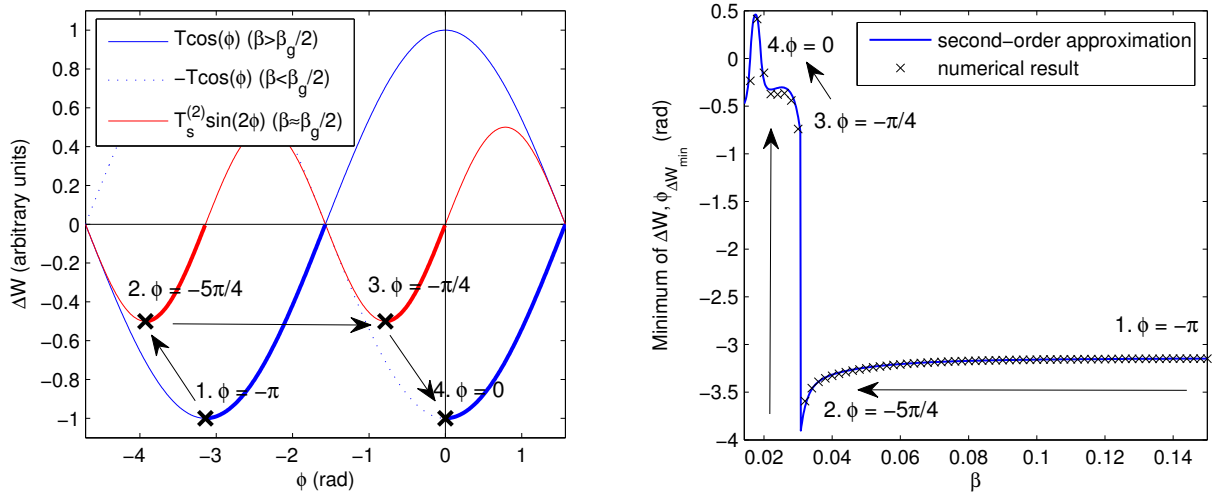

(a) Schematic.

(b) Phase of the minimum of ΔW.

Figure 5: Phasing the low-β cavity for deceleration ($A/q = 4.5$ and $E_0 = 6$ MV/m).

is neglected in the schematic of Figure 5(a). An analytic understanding of the phase dependence of the energy gain at low velocity is important for maintaining the phase stability of the beam.

5.2 Example: deceleration in the HIE-ISOLDE linac

The heaviest beams with $A/q = 4.5$ can be decelerated down to 0.45 MeV/u at a synchronous phase with respect to the minimum of the energy gain of $\phi_s = +20°$ where,

$$\phi(\beta) = \phi_{\Delta W_{\min}}(\beta) + \phi_s, \tag{11}$$

which is equivalent to $-160°$ in the first-order approximation. The deceleration in this case is limited by the number of low-β cavities. The 12 superconducting low-β cavities provide an effective deceleration potential of 3.4 MV for $A/q = 4.5$ and 3.0 MV for $A/q = 3$, as opposed to 10.8 MV for acceleration. The beam energy after each cavity is shown in Figure 6 using the first and second-order approximations with a comparison made to the numerical result and the TRACK code [6] for two beams with $A/q = 4.5$ and 3.

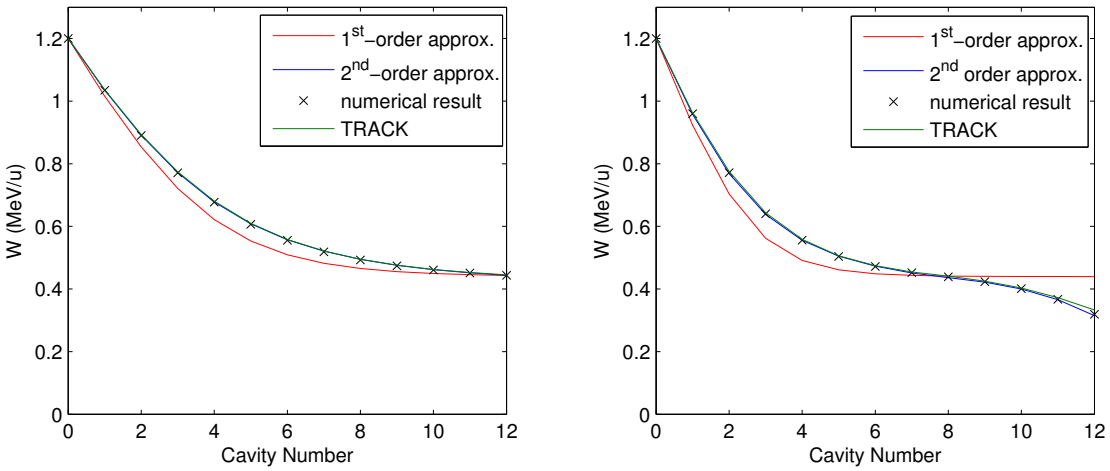

(a) $A/q = 4.5$. (b) $A/q = 3$.

Figure 6: Deceleration in the low energy section ($E_{\text{acc}} = 6$ MV/m and $\phi_s = +20°$).

The phase dependence of the energy gain in the cavities is shown explicitly in Figures 7 and 8 for decelerating beams with $A/q = 4.5$ and 3, respectively. The linear regions become much smaller as the velocity tends towards $\beta_g/2$, which is the limiting factor for the longitudinal beam quality when decelerating. The final subplot in each figure shows an expanded scale highlighting the reliability of the second-order approximation, even at low velocity.

6 Conclusion

Analytic approximations to the second-order transit-time factors were derived and compared to those calculated with the realistic field profile. The square-wave approximation breaks down most severely for the first-order transit-time factor. Therefore, the realistic fields should be used to calculate the transit-time factors for $\beta \ll \beta_g$. The second-order formalism was used to accurately describe the longitudinal dynamics during deceleration in the low-β cavities of the HIE-ISOLDE linac and was shown to be a quick and easy method for calculating the phases of the cavities.

7 Acknowledgements

The author would like to thank Jean Delayen for his help in deriving the above formulae and demonstrating the derivation of the second-order transit-time factors for a single gap, which are stated for reference in Appendix C [7].

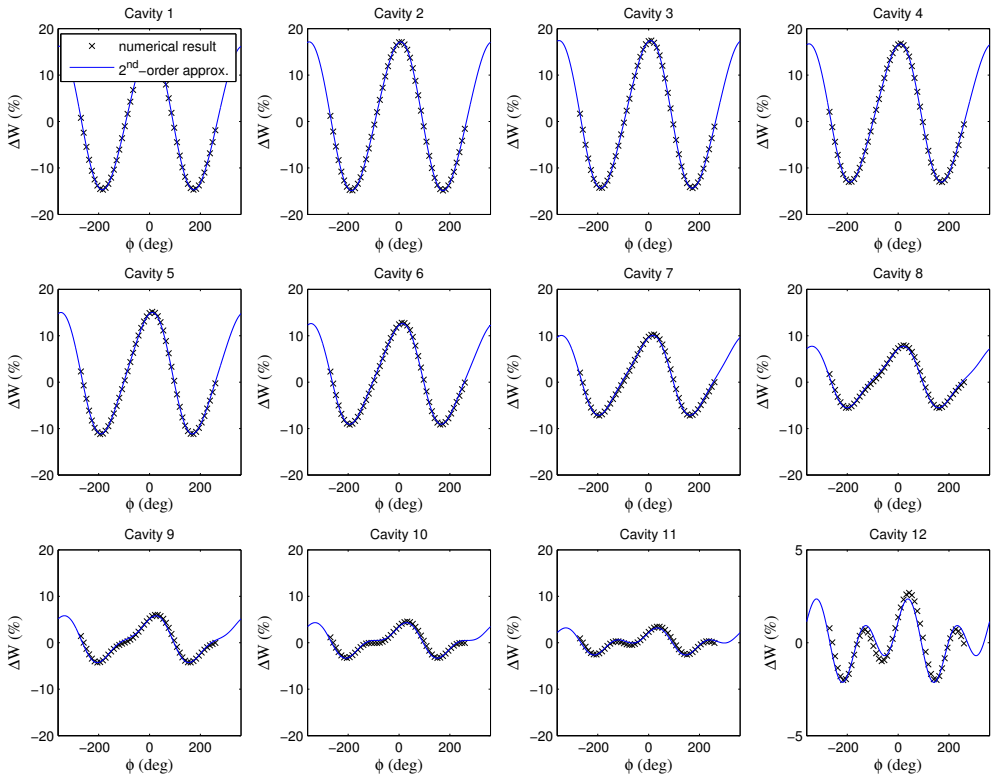

Figure 7: ΔW vs. ϕ in the low-β cavities of the HIE-ISOLDE linac whilst decelerating with $A/q = 4.5$.

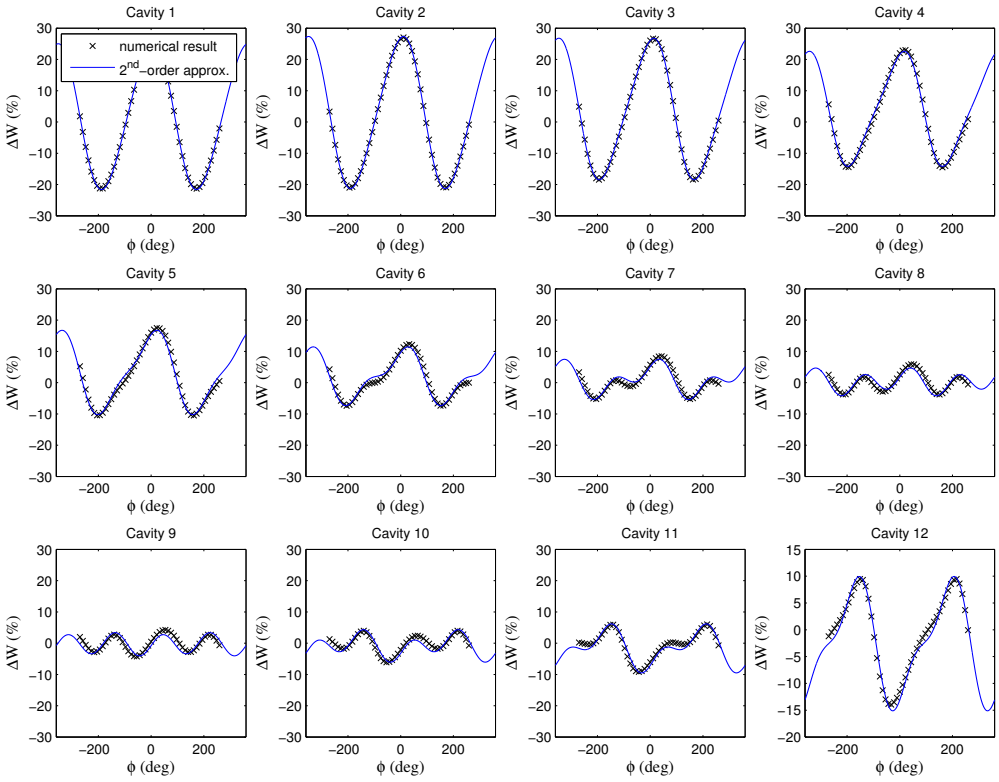

Figure 8: ΔW vs. ϕ in the low-β cavities of the HIE-ISOLDE linac whilst decelerating with $A/q = 3$.

Appendices

A Derivation of $\hat{\mathbf{T}}^{(\mathbf{2})}$ for a Two Gap Resonator

First, rewrite the expression for the first-order transit-time factor in a simpler form:

$$\hat{T}_{2\,gap}(x) = \frac{\sin x}{x} \sin \alpha x,$$

where,

$$x = \frac{\pi g}{\beta \lambda},$$

and,

$$\alpha = \frac{\beta_g \lambda}{2g} = \frac{L}{g}.$$

The derivation is straightforward:

$$\hat{T}'_{2\,gap}(x) = \frac{\mathrm{d}}{\mathrm{d}x}\hat{T}_{2\,gap}(x) = \frac{1}{x}\left[\cos x \sin \alpha x + \alpha \sin x \cos \alpha x - \hat{T}_{2\,gap}(x)\right].$$

Using,

$$\hat{T}^{(2)}_{2\,gap}(x) = -\frac{x}{4}\hat{T}_{2\,gap}(x)\hat{T}'_{2\,gap}(x),$$

implies that,

$$\hat{T}^{(2)}_{2\,gap}(x) = -\frac{\hat{T}_{2\,gap}(x)}{4}\left[\cos x \sin \alpha x + \alpha \sin x \cos \alpha x - \hat{T}_{2\,gap}(x)\right].$$

B Derivation of $\hat{\mathbf{T}}^{(\mathbf{2})}_{\mathbf{s}}$ for a Two Gap Resonator

First, separate the integral into two parts, I and II:

$$\begin{aligned}\hat{T}^{(2)}_{s,2\,gap} &= -\frac{x}{8\pi}\int_{-\infty}^{+\infty} \frac{\hat{T}'_{2\,gap}(x+x')\hat{T}_{2\,gap}(x-x') - \hat{T}_{2\,gap}(x+x')\hat{T}'_{2\,gap}(x-x')}{x'}\,\mathrm{d}x' \\ &= -\frac{x}{8\pi}\int_{-\infty}^{+\infty} \underbrace{\frac{\hat{T}'_{2\,gap}(x+x')\hat{T}_{2\,gap}(x-x')}{x'}}_{\text{I}} - \underbrace{\frac{\hat{T}_{2\,gap}(x+x')\hat{T}'_{2\,gap}(x-x'))}{x'}}_{\text{II}}\,\mathrm{d}x'.\end{aligned}$$

Focusing on simplifying the expressions inside the integral, I can be expressed as:

$$\begin{aligned}\mathrm{I} = &\underbrace{\frac{1}{x'(x^2-x'^2)}\sin(x-x')\cos(x+x')\sin(\alpha(x+x'))\sin(\alpha(x-x'))}_{\text{a}} \\ &+\underbrace{\frac{\alpha}{x'(x^2-x'^2)}\sin(x-x')\sin(x+x')\sin(\alpha(x-x'))\cos(\alpha(x+x'))}_{\text{b}} \\ &-\underbrace{\frac{1}{x'(x+x')(x^2-x'^2)}\sin(x-x')\sin(x+x')\sin(\alpha(x-x'))\sin(\alpha(x+x'))}_{\text{c}}.\end{aligned}$$

Similarly, II can be expressed as:

$$\begin{aligned}\mathrm{II} = &\underbrace{\frac{1}{x'(x^2-x'^2)}\sin(x+x')\cos(x-x')\sin(\alpha(x+x'))\sin(\alpha(x-x'))}_{\text{a}} \\ &+\underbrace{\frac{\alpha}{x'(x^2-x'^2)}\sin(x-x')\sin(x+x')\sin(\alpha(x+x'))\cos(\alpha(x-x'))}_{\text{b}} \\ &-\underbrace{\frac{1}{x'(x-x')(x^2-x'^2)}\sin(x-x')\sin(x+x')\sin(\alpha(x-x'))\sin(\alpha(x+x'))}_{\text{c}}.\end{aligned}$$

Considering pairs of terms separately and using the trigonometric identities quoted, $\mathrm{I.a}-\mathrm{II.a}$ can be written:

$$\begin{aligned}\mathrm{I.a}-\mathrm{II.a} &= \frac{\overbrace{\sin(\alpha(x-x'))\sin(\alpha(x+x'))}^{\frac{\cos(2\alpha x')-\cos(2\alpha x)}{2}}}{x'(x^2-x'^2)}\underbrace{[\sin(x-x')\cos(x+x')-\sin(x+x')\cos(x-x')]}_{\sin(-2x')} \\ &= \frac{\cos(2\alpha x)\sin(2x')}{2x'(x^2-x'^2)}-\frac{\sin(2x')\cos(2\alpha x')}{2x'(x^2-x'^2)}.\end{aligned}$$

$\mathrm{I.b}-\mathrm{II.b}$ can be written:

$$\begin{aligned}\mathrm{I.b}-\mathrm{II.b} &= \frac{\alpha\overbrace{\sin(x-x')\sin(x+x')}^{\frac{\cos(2x')-\cos(2x)}{2}}}{x'(x^2-x'^2)}\underbrace{[\sin(\alpha(x-x'))\cos(\alpha(x+x'))-\sin(\alpha(x+x'))\cos(\alpha(x-x'))]}_{\sin(-2\alpha x')} \\ &= \frac{\alpha\cos(2x)\sin(2\alpha x')}{2x'(x^2-x'^2)}-\frac{\alpha\sin(2\alpha x')\cos(2x')}{2x'(x^2-x'^2)}.\end{aligned}$$

And, $\mathrm{I.c}-\mathrm{II.c}$ can be written:

$$\text{I.c} - \text{II.c} = \overbrace{\left[\frac{1}{x-x'} - \frac{1}{x+x'}\right]}^{\frac{2x'}{x^2-x'^2}} \overbrace{\frac{\sin(x-x')\sin(x+x')}{2}}^{\frac{\cos(2x')-\cos(2x)}{2}} \overbrace{\frac{\sin(\alpha(x-x'))\sin(\alpha(x+x'))}{2}}^{\frac{\cos(2\alpha x')-\cos(2\alpha x)}{2}} \frac{}{x'(x^2-x'^2)}$$
$$= \frac{\cos(2x')\cos(2\alpha x')}{2(x^2-x'^2)^2} - \frac{\cos(2\alpha x)\cos(2x')}{2(x^2-x'^2)^2} - \frac{\cos(2x)\cos(2\alpha x')}{2(x^2-x'^2)^2} + \frac{\cos(2x)\cos(2\alpha x)}{2(x^2-x'^2)^2}.$$

These expressions can then be integrated using the standard integrals included in Appendix D. The terms denoted, a, give:

$$-\frac{x}{8\pi}\int_{-\infty}^{+\infty}(\text{I.a} - \text{II.a})\,\mathrm{d}x' = \frac{x}{16\pi}\underbrace{\int_{-\infty}^{+\infty}\frac{\sin(2x')\cos(2\alpha x')}{x'(x^2-x'^2)}\,\mathrm{d}x'}_{\int \#3(b>a)} - \frac{x\cos(2\alpha x)}{16\pi}\underbrace{\int_{-\infty}^{+\infty}\frac{\sin(2x')}{x'(x^2-x'^2)}\,\mathrm{d}x'}_{\int \#4}$$
$$= \frac{x}{16\pi}\left[\frac{\pi\sin 2x\sin 2\alpha x}{x^2}\right] - \frac{x\cos 2\alpha x}{16\pi}\left[\frac{\pi(1-\cos 2x)}{x^2}\right]$$
$$= \frac{1}{16x}\left[\sin 2x\sin 2\alpha x - (1-\cos 2x)\cos 2\alpha x\right]. \tag{12}$$

The terms denoted, b, give:

$$-\frac{x}{8\pi}\int_{-\infty}^{+\infty}(\text{I.b} - \text{II.b})\,\mathrm{d}x' = \frac{\alpha x}{16\pi}\underbrace{\int_{-\infty}^{+\infty}\frac{\sin(2\alpha x')\cos(2x')}{x'(x^2-x'^2)}\,\mathrm{d}x'}_{\int \#3(a>b)} - \frac{\alpha x\cos(2x)}{16\pi}\underbrace{\int_{-\infty}^{+\infty}\frac{\sin(2\alpha x')}{x'(x^2-x'^2)}\,\mathrm{d}x'}_{\int \#4}$$
$$= \frac{\alpha x}{16\pi}\left[\frac{\pi(1-\cos 2x\cos 2\alpha x)}{x^2}\right] - \frac{\alpha x\cos 2x}{16\pi}\left[\frac{\pi(1-\cos 2\alpha x)}{x^2}\right]$$
$$= \frac{\alpha}{16x}\left[1-\cos 2x\right]. \tag{13}$$

And the terms denoted, c, give:

$$-\frac{x}{8\pi}\int_{-\infty}^{+\infty}(\text{I.c} - \text{II.c})\,\mathrm{d}x' = -\frac{x}{16\pi}\underbrace{\int_{-\infty}^{+\infty}\frac{\cos(2x')\cos(2\alpha x')}{(x^2-x'^2)^2}\,\mathrm{d}x'}_{\int \#5}$$
$$+\frac{x\cos(2\alpha x)}{16\pi}\underbrace{\int_{-\infty}^{+\infty}\frac{\cos(2x')}{(x^2-x'^2)^2}\,\mathrm{d}x'}_{\int \#6}$$
$$+\frac{x\cos(2x)}{16\pi}\underbrace{\int_{-\infty}^{+\infty}\frac{\cos(2\alpha x')}{(x^2-x'^2)^2}\,\mathrm{d}x'}_{\int \#6}$$
$$-\frac{x\cos(2x)\cos(2\alpha x)}{16\pi}\underbrace{\int_{-\infty}^{+\infty}\frac{1}{(x^2-x'^2)^2}\,\mathrm{d}x'}_{\int \#7}$$

$$= -\frac{x}{16\pi}\left[\frac{\pi}{2x^3}\{-2\alpha x\cos(2\alpha x)\cos(2x)+\sin(2\alpha x)(\cos(2x)+2x\sin(2x))\}\right] + \frac{x\cos(2\alpha x)}{16\pi}\left[\frac{\pi}{2x^3}\sin(2x)-2x\cos(2x)\right] + \frac{x\cos(2x)}{16\pi}\left[\frac{\pi}{2x^3}\sin(2\alpha x)-2\alpha x\cos(2\alpha x)\right]$$

$$= \frac{1}{16x^2}\left[\frac{\sin 2x\cos 2\alpha x}{2} - x(\sin 2x\sin 2\alpha x+\cos 2x\cos 2\alpha x)\right]. \tag{14}$$

Finally, the derivation is completed by putting parts I and II together and summing Equations 12, 13 and 14. Therefore,

$$\hat{T}^{(2)}_{s,2\,gap} = \frac{\alpha x}{8}\frac{\sin^2 x}{x^2} + \frac{\cos 2\alpha x}{16x}\left[\frac{\sin 2x}{2x}-1\right].$$

The result can be rewritten in terms of the single gap transit-time factor,

$$\hat{T}^{(2)}_{s,2\,gap} = \frac{\alpha x}{8}\hat{T}^2_{1\,gap}(x) + \frac{\cos 2\alpha x}{16x}\left[\hat{T}_{1\,gap}(2x)-1\right].$$

C $\hat{\mathbf{T}}^{(2)}$ and $\hat{\mathbf{T}}^{(2)}_{\mathbf{s}}$ for a Single Gap Resonator

The second-order transit-time factors for a two-gap resonator can be compared to those for a single gap shown below [7],

$$\hat{T}^{(2)}_{1\,gap}(x) = -\frac{\hat{T}_{1\,gap}(x)}{4}\left[\cos x-\hat{T}_{1\,gap}(x)\right] \quad \text{and} \quad \hat{T}^{(2)}_{s,1\,gap}(x) = \frac{1}{8x}\left[1-\hat{T}_{1\,gap}(2x)\right],$$

where,

$$\hat{T}_{1\,gap}(x) = \frac{\sin x}{x}.$$

D Standard Integrals

The standard integrals were found in the tables of Gradshteyn and Ryzhik [8]. The equation reference numbers are also quoted.

$$\int \#1 : (3.741.2) :$$

$$\int_{-\infty}^{+\infty} \frac{\sin(ax)\cos(bx)}{x}\,\mathrm{d}x = \begin{cases} \pi & \text{if } a > b \geq 0 \\ \frac{\pi}{2} & \text{if } a = b \geq 0 \\ 0 & \text{if } b > a \geq 0 \end{cases}$$

$$\int \#2 : (3.742.7) :$$

$$\int_{-\infty}^{+\infty} \frac{x\sin(ax)\cos(bx)}{c^2 - x^2}\,\mathrm{d}x = \begin{cases} -\pi\cos(ac)\cos(bc) & \text{if } a > b > 0 \\ -\frac{\pi}{2}\cos(2ac) & \text{if } a = b \geq 0 \\ \pi\sin(ac)\sin(bc) & \text{if } b > a > 0 \end{cases}$$

$$\int \#3 :$$

$$\int_{-\infty}^{+\infty} \frac{\sin(ax)\cos(bx)}{x(c^2 - x^2)}\,\mathrm{d}x = \frac{1}{c^2}\underbrace{\int_{-\infty}^{+\infty} \frac{\sin(ax)\cos(bx)}{x}\,\mathrm{d}x}_{\int \#1} + \frac{1}{c^2}\underbrace{\int_{-\infty}^{+\infty} \frac{x\sin(ax)\cos(bx)}{c^2 - x^2}\,\mathrm{d}x}_{\int \#2}$$

$$= \begin{cases} \frac{\pi}{c^2}(1 - \cos(ac)\cos(bc)) & \text{if } a > b > 0 \\ \frac{\pi}{c^2}\sin(ac)\sin(bc) & \text{if } b > a > 0 \\ -\frac{\pi}{4}\cos(2ac) & \text{if } a = b \geq 0 \end{cases}$$

$$\int \#4 : (3.725.2) :$$

$$\int_{-\infty}^{+\infty} \frac{\sin(ax)}{x(b^2 - x^2)}\,\mathrm{d}x = \frac{\pi}{b^2}(1 - \cos ab).$$

$$\int \#5 : (3.728.5) :$$

$$\lim_{c \to b} \int_{-\infty}^{+\infty} \frac{\cos(ax)}{(b^2 - x^2)(c^2 - x^2)}\,\mathrm{d}x = \int_{-\infty}^{+\infty} \frac{\cos(ax)}{(b^2 - x^2)^2}\,\mathrm{d}x = \frac{\pi}{2b^3}\left[\sin(ab) - ab\cos(ab)\right].$$

$$\int \#6 : (3.728.5) :$$

$$\lim_{c\to b}\int_{-\infty}^{+\infty} \frac{\cos(ax)}{(b^2-x^2)(c^2-x^2)}\,\mathrm{d}x = \int_{-\infty}^{+\infty} \frac{\cos(ax)}{(b^2-x^2)^2}\,\mathrm{d}x = \frac{\pi}{2b^3}\left[\sin(ab) - ab\cos(ab)\right].$$

$$\int \#7 : (2.172) \text{ and } (2.173.1) :$$

$$\int_{-\infty}^{+\infty} \frac{1}{(a^2-x^2)^2}\,\mathrm{d}x = 0.$$

References

[1] J.R. Delayen, *Nucl. Instrum. Meth. A* **258**, 15-25, 1987.

[2] M.A. Fraser, *et al.*, Beam Dynamics Studies for the HIE-ISOLDE Linac at CERN, Proc. of PAC 2009, Vancouver.

[3] M. Pasini, *et al.*, HIE-ISOLDE: The Superconducting RIB Linac at CERN, Proc. of SRF Conference 2009, Berlin.

[4] A. D'Elia, *et al.*, HIE-ISOLDE High-beta Cavity Study and Measurements, Proc. of SRF Conference 2009, Berlin.

[5] M.A. Fraser, *et al.*, Compensation of Transverse Field Asymmetry in the High-beta Quarter-wave Resonator of the HIE-ISOLDE Linac at CERN, Proc. of SRF Conference 2009, Berlin.

[6] P.N. Ostroumov, V. Aseev, and B. Mustapha, `TRACK` - a Code for Beam Dynamics Simulation in Accelerators and Transport Lines with 3D Electric and Magnetic Fields, ANL, Argonne, IL, USA, v. 37 ed. (2007) (http:// www.phy.anl.gov/atlas/TRACK/).

[7] J.R. Delayen, Private communication, 2009.

[8] I.S. Gradshteyn and I.M. Ryzhik, Table of Integrals, Series and Products (Fifth Edition), Academic Press, 1994.

[9] Wolfram Mathematica v 7.0.1.0, `http://www.wolfram.com`.